Journal of Hazardous Materials 211–212 (2012) 247–254

Contents lists available at SciVerse ScienceDirect

Journal of Hazardous Materials

journal homepage: www.elsevier.com/locate/jhazmat

Reduction of carbon dioxide on jet spray formed titanium dioxide surfaces

J.W. MacFarlane*, T.B. Scott

Interface Analysis Centre, Oldbury House, 121 St. Michael's Hill, Bristol BS2 8BS, United Kingdom

ARTICLE INFO

Article history:
Received 11 June 2011
Received in revised form 9 August 2011
Accepted 7 September 2011
Available online 14 September 2011

Keywords:
Titania
Titanium dioxide
Carbon dioxide
Fixation
X-ray activation
X-ray irradiation

ABSTRACT

The photocatalytic reduction of carbon dioxide (CO_2) on jet spray formed titanium dioxide (TiO_2) was studied using light-emitting diode (LED) illumination centred at a wavelength of 388 nm. In addition, the photocatalytic reduction of CO_2 under soft X-ray irradiation was also studied. Specifically, the experiments examined the reduction of CO_2 in a gaseous and liquid–gas system using residual gas analysis mass spectrometry. A photochemical reduction of CO_2 was observed over a course of 250 min, with transformation to a major product, $C_2H_3O^-$ (ethenolate), until equilibrium was reached. The product was observed to be surface stabilised, with it reverting back to CO_2 over the course of 100 min without illumination. A proposed free radical mechanism is presented for the formation of this product. A similar effect to that of UV illumination is also observed to occur under the influence of soft X-rays, which presents a potentially significant alternative method for the activation of TiO_2.

1. Introduction

Greenhouse gases such as CO_2, CH_4, CFCs and NO_x are being released in increasing quantities worldwide and have been linked to anthropogenic climate change [1]. These are of serious environmental concern with research suggesting melting ice caps, rise in sea level and a reduction in biodiversity from the climate change in the next century [2]. Although gasses such as CH_4 have a greater heating effect per mole of substance, research has been primarily focused on CO_2 due to its long atmospheric life time, and high rates of emission. Significant research effort has focused on methods to reduce the amount of CO_2 released and also develop procedures to remove excess CO_2 from the atmosphere. Several different storage techniques have been proposed, for example: storage in soils; fixation in obsolete oil wells; or mineralisation within mafic rocks [3]. An area that has received relatively less attention is the use of photocatalytic semiconductors such as TiO_2 for the chemical reduction of CO_2 [4–8]. Conceptually, the reaction products, such as ethanol, can then be stored, used as a fuel source or polymerised to be used in the plastics industry. With peak oil predicted to occur within 30 years [3] a method of transforming CO_2 into an alternative fuel source would have significant value [9].

Furthermore, with the signing of the Kyoto protocol, many countries have agreed to reduce CO_2 emissions to 5% below 1990 levels [10]. Accordingly the evolution of a new market in carbon trading has developed [3,11]. Carbon trading enables governments to offset overproduction of CO_2 via trading with under-producing nations to avoid economic penalisation. Thus technology to enable a country to reduce its CO_2 emissions without cutting fossil fuel consumption is highly desirable.

TiO_2 worldwide annual production exceeds 5.5×10^{12} tonnes, and is commercially inexpensive [12]. It is widely used as a pigment, is a permitted food colouring as E171 and is a common component in sun screen products. The surface photocatalytic oxidation mechanism of semiconductors with adsorbed water is well documented [12,13]. Upon the illumination of TiO_2 surfaces, with light of wavelength <388 nm, electrons are promoted from the valence band to the conduction band. This leaves a corresponding hole (h^+_{vb}) upon the surface of the material which reacts with adsorbed H_2O generating reactive oxygen species (ROS) (1).

$$TiO_2 \xrightarrow{h\nu} h^+_{vb} + e^-_{cb} \quad (1a)$$

$$h^+_{vb} + H_2O \longrightarrow {}^\bullet OH + H^+ \quad (1b)$$

$$e^-_{cb} + H^+ \longrightarrow {}^\bullet H \quad (1c)$$

The ROS can in turn oxidise and reduce surface bonded compounds and provide a possible mechanism for the reduction of CO_2. Previous studies have examined CO_2 saturated aqueous suspensions of TiO_2 nanoparticles [14], or free nanoparticles [4–8]. Here we demonstrate with use of residual gas analysis mass spectrometry intermediate reactant products present in the system, and the effectiveness of jet sprayed TiO_2 for the chemical reduction of CO_2 in the gaseous phase.

* Corresponding author. Tel.: +44 0117 331 1171; fax: +44 0117 331 1171.
E-mail address: james.macfarlane@bristol.ac.uk (J.W. MacFarlane).

0304-3894/$ – see front matter © 2011 Elsevier B.V. All rights reserved.
doi:10.1016/j.jhazmat.2011.09.026

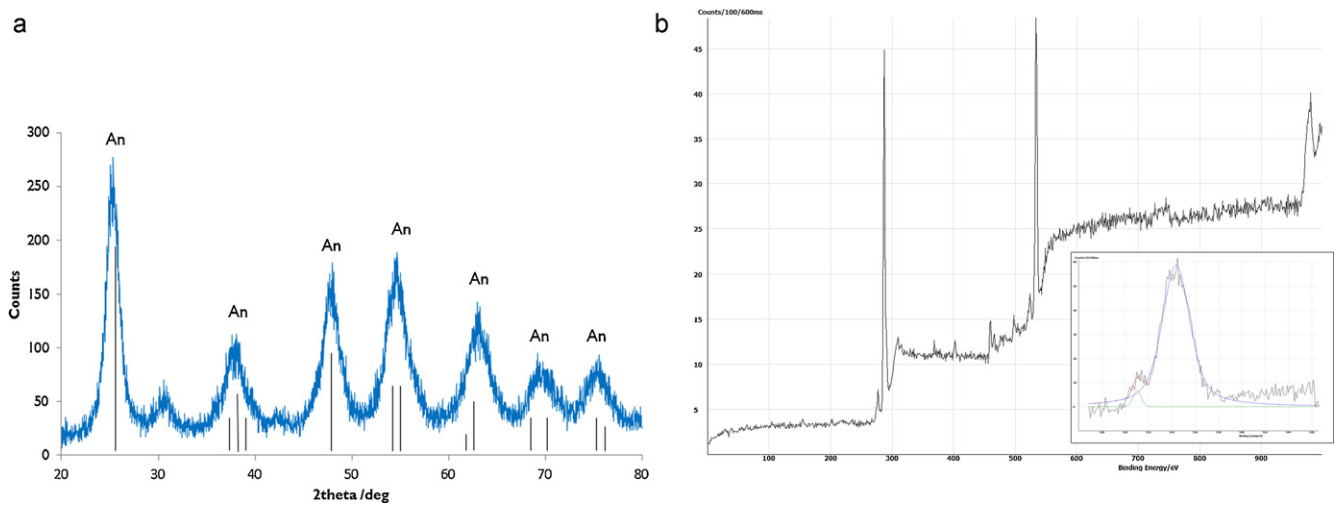

Fig. 1. XRD (a) and XPS (b) data of surface with insert showing bonded H_2O. XRD data shows a strong anatase signal, and XPS illustrates the presence of both physi- and chemisorbed water.

2. Materials and methods

2.1. Photocatalysts

Photocatalytic surfaces used in this study, kindly donated by the University of Aveiro Portugal, were prepared via a jet spray screen printing method. Commercial TiO_2 nano-particles (Kronos), suspended in an organic medium (1:1 wt%), were deposited upon an aluminium substrate and heated to 450 °C in order to crystallize the surface. A full description of the formation method can be found in the literature [15]. The surfaces produced exhibited a high surface area (13.72 $m^2\ g^{-1}$) and were physically stable, uniform and robust. Preliminary X-ray diffraction (XRD) analysis confirmed that the TiO_2 was in the anatase form, whilst X-ray photoelectron spectroscopy (XPS) was used to examine the surface chemistry of the coating and confirmed the presence of both physi- and chemisorbed water (Fig. 1). The UV light source implemented in this study was a specifically developed 40 W light-emitting diode (LED) experimentally determined to emit at 388 nm (W.N. Wang, University of Bath).

2.2. Reaction vessel

The batch system for exposing the TiO_2 coatings to the reactants was set up as illustrated in the simplified schematic, Fig. 2.

A sealed stainless steel reaction vessel of 590 cm^3 internal volume was used to house each experiment and was fitted with a UV transmitting window. The vessel was directly connected to a residual gas analysis (RGA) mass spectrometer (e-Vision, MKS Instruments) and associated pumping system, via a sapphire leak valve, such that gaseous species in the reaction vessel could be sampled without any significant volume loss. 75 $cm^3\ min^{-1}$ of CO_2 (99.8% pure, obtained from Air Products) was bubbled through distilled water to provide a high humidity environment within the reaction vessel. The system was flushed out in this manner for 30 min, then the reaction vessel isolated. Samples where illuminated using a 40 W LED, and shielded from external light sources. The RGA mass spectrometer was operated at a working pressure of 4.0×10^{-5} mbar. Gas samples were both taken continuously to analyse the compositional changes with time, over a course of up to 48 h. Furthermore all samples were run under continuous LED illumination unless specifically stated otherwise. All experiments were performed in an air conditioned laboratory, with a working temperature of 290 K, however, no active method was employed to control the absolute temperature within the reaction vessel.

2.3. Experimental method

Three main experiments where performed, with multiple repeats to ensure consistency of results. In the first experiment, the

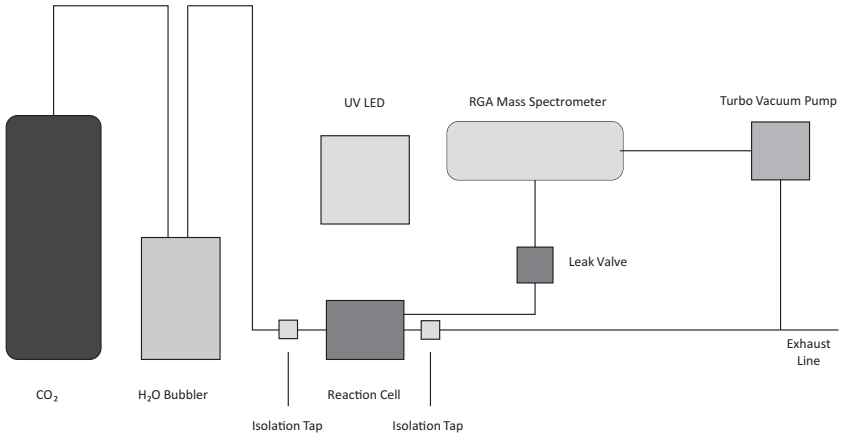

Fig. 2. Simplified schematic diagram of experimental setup, consisting of a stainless steel reaction vessel connected via a sapphire leak valve to a residual gas analysis mass spectrometer. UV illumination is provided via a high power LED light source.

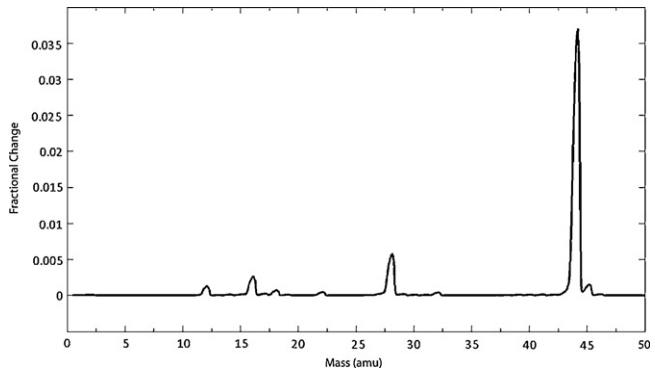

Fig. 3. The initial gas composition of the cell analysed by residual gas mass spectrometry. Peak heights express the fraction that each peak contributes to the total signal. A fractional composition can be calculated by taking the area of each peak.

stainless steel reaction cell was filled with wet CO_2 and then subsequently sealed as a fixed volume. The wet CO_2 was generated by bubbling CO_2 through deionised water which was passed through the reaction cell at a constant rate of 100 cm^3 min^{-1} for 15 min before being sealed. Prior to UV illumination, the gas composition of the cell was monitored over a 10 min period to determine the initial baseline composition.

In the second set of experiments, the reaction vessel was half filled with deionised H_2O. This mixed-phase system was cycled by washing the H_2O over the sample surface. The sample, mounted vertically and at mid height within the reaction cell, was continuously washed with a flow of water droplets from height (65 cm^3 min^{-1}), which then ponded into a lower reservoir within the cell. Total H_2O in the system occupied 27% (160 ml) of the reaction cell.

In the third set of experiments, a wet CO_2 system was investigated but the UV source was replaced with a Cr Kα X-ray source. The quartz reaction vessel window was replaced with beryllium, to allow for the propagation of X-rays to the sample. Samples were analysed for a duration of 3 h with RGA data continuously recorded.

Control experiments (without UV or X-ray illumination) were performed for comparison, but exhibited no detectable changes in gas composition, above instrument noise, over the course of the experiment.

The initial gas composition within the reaction cells for each of the experiments was equivalent and can be seen in Fig. 3. Within the system the masses of the predominant species detected were recorded at 44 amu (CO_2 – 90%), 28 amu (CO, or CO_2^{2+}), 16 amu (O) and 12 amu (C). Trace amounts of H_2O were also detected in the gas phase, equivalent to approximately 19 mbar water vapour pressure in the reaction cell.

2.4. Data processing

In order to identify any changes in system gas composition over time the following data processing was performed. The RGA data

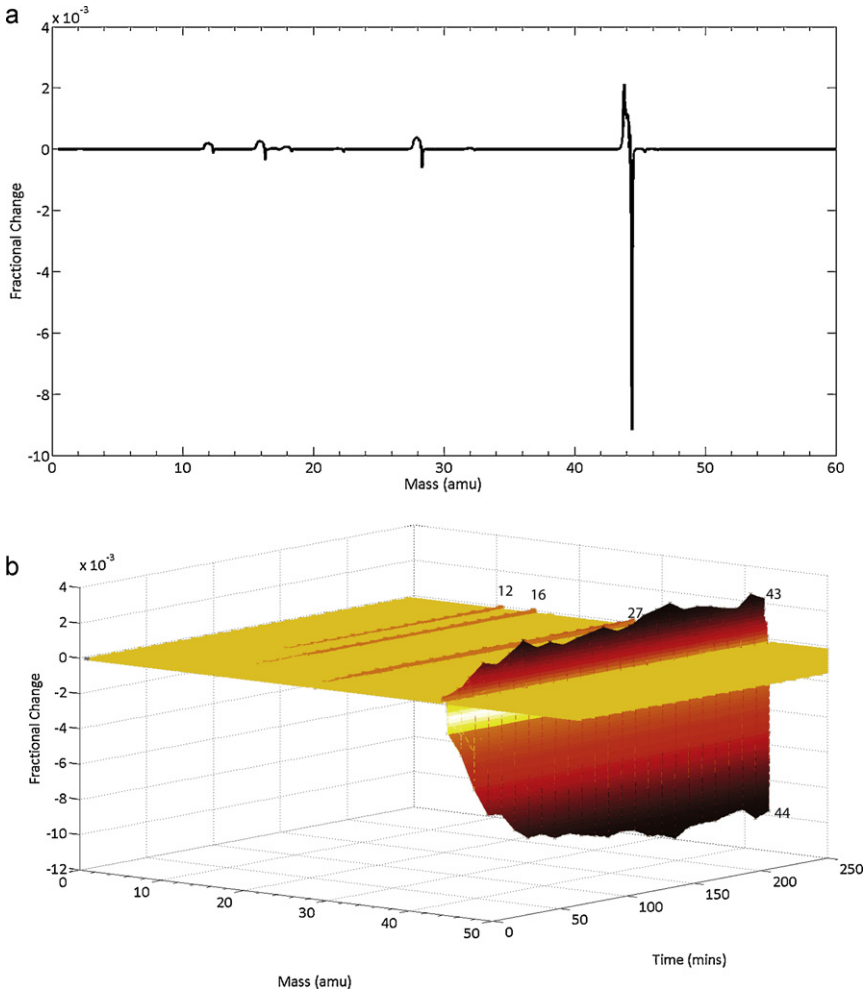

Fig. 4. The change in gas composition over time. The 2D slice (a) shows the compositional change after 250 min of illumination. The 3D image (b) is included to give some indication of the reaction kinetics over the course of illumination.

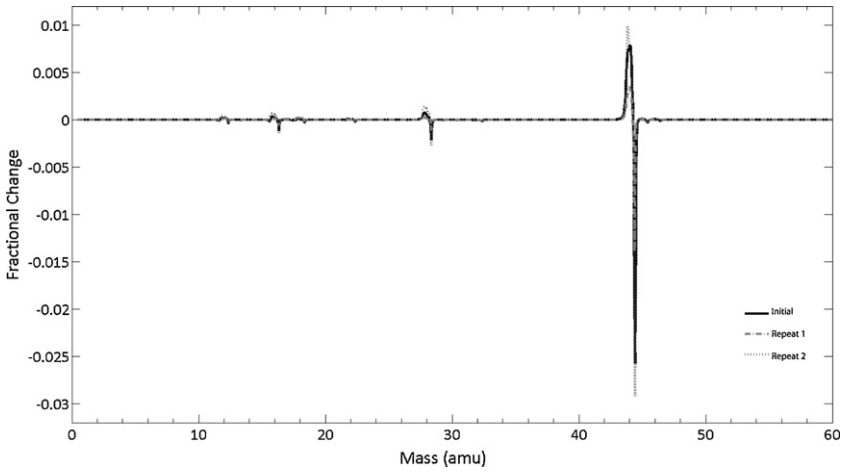

Fig. 5. Showing the changes in gas composition over time. The multiple samples show high concordance.

was collected continuously, scanning over a range of 0–50 amu with a step size of 0.3 amu. The raw signal, recording partial pressure as a function of mass, was converted to the fractional amount of mass within the system. The average gas composition determined over the initial 10 min sampling period without UV or X-ray illumination, was subtracted as a background from the remaining data to highlight temporal changes in the gas composition. A typical example of processed data can be seen in Fig. 4 with 3D plots used to illustrated the change in composition over time, and a 2D slice removed at $t = 250$ min, in order to better show the change in composition. The format for all subsequent figures follows the above stated configuration.

3. Results

3.1. Compositional changes in gas chemistry

The results of residual gas analysis provided clear evidence for the photocatalytic reduction of CO_2 during sample illumination by both UV and soft X-rays. For experiment 1, which investigated a wet CO_2 system under UV illumination, the change in gas composition after 250 min of illumination with three repeats is shown in Fig. 5. Increases at m/z values of 12, 16, 18, 27, and 43 and major decreases at 28, and 44 were recorded, indicating a significant change in gas composition with the system. Detailed peak analysis indicated that there was no change in the total gas pressure over the course of the experiment. The intensity decrease of the recorded mass peak at 44 amu (ascribed to CO_2) was observed to account for 90% of the total observed mass peak decreases. Concurrently the most abundant species produced during the experiment was at 43 amu, accounting for 40% of all mass peak increases. The recorded decrease in CO_2 equated to approximately a 10% net decrease in the total amount of CO_2 within the system. This can be calculated approximately as 0.024 mol of CO_2 uptake over the time period. Scaling appropriately this equates to a CO_2 fixation rate of 240 mol m^{-2} of sample over the 4 h period. Concurrently 0.002 mol of the product at 43 amu was generated over the time period equivalent to 100 mol m^{-2} of surface.

Fig. 6 illustrates the volatile compositional changes of the system during the course of illumination when the surface is washed with H_2O. Although the main changes to the mass peaks remain similar, the reduction in CO_2 is slightly less, and the reduction of CO is enhanced. This is likely to be appertained to CO_2 dissolution in H_2O, and the chemically buffered scenario this creates. The mass peak at 43 amu, ascribed as the principle reaction product was found to have twice the intensity, indicating a greater reaction efficacy. Coupled with this, catalyst poisoning was observed to occur at an enhanced rate.

From the above system a water sample was removed after 48 h of illumination, in order to gain a better understanding of the reaction product. The sample was agitated and slightly warmed, in order to increase the partial pressure of the volatile organics within the head space. The spectrum of which can be seen in Fig. 7.

Fig. 8 shows the influence of X-ray irradiation on the gaseous sample system. A comparable spectrum to that recorded for UV illumination was observed, although some minor variations in the signal exist. A significant increase at mass 27 is observed along with a major decrease at 28 amu. The reaction rates, and percentages of products formed appear similar to these observed under UV illuminated samples.

In order to assess the stability of the formed products, a sample was illuminated as above for 8 h. After this time period illumination ceased, and the vessel remained sealed. It was observed that the reaction product of mass 43 amu gradually disappeared over the course of 100 min, Fig. 9, although some stable bi-products remained (C, CH_4, CO). It is indicated that there is a net overall decrease in the amount of CO_2 within the system, suggesting that the reactive intermediates are stable.

In all of the above experiments, good concordance between repeat samples was observed, with no statistically significant deviations observed.

4. Discussion

4.1. Formation products

Increases at masses 12, 16, 18, 27, 43 and decreases at 28, and 44 amu are seen with illumination. C (12), O(16), H_2O (18), C_2H_3 (27), $C_2H_3O^-$ (43) are ascribed to the increases, and CO^{2+} (28) and CO_2 (44) to the decrease. Fig. 7 shows the composition of the volatile organic (mass 43 amu) formed during the experiments. Major electron impact (EI) ionization splitting peaks are ascribed to C_2H_3 (27), CO (28), CH_3O (31) and $C_2H_3O^-$ (43). The major product appears surface stabilised and is discussed below. During the course of the experiment, poisoning of the catalysis occurs, with the deposition of solid C onto the TiO_2 surface. The deposition of the carbon is relatively slow, with noticeable change only after 200 h, and was confirmed using EDX analysis.

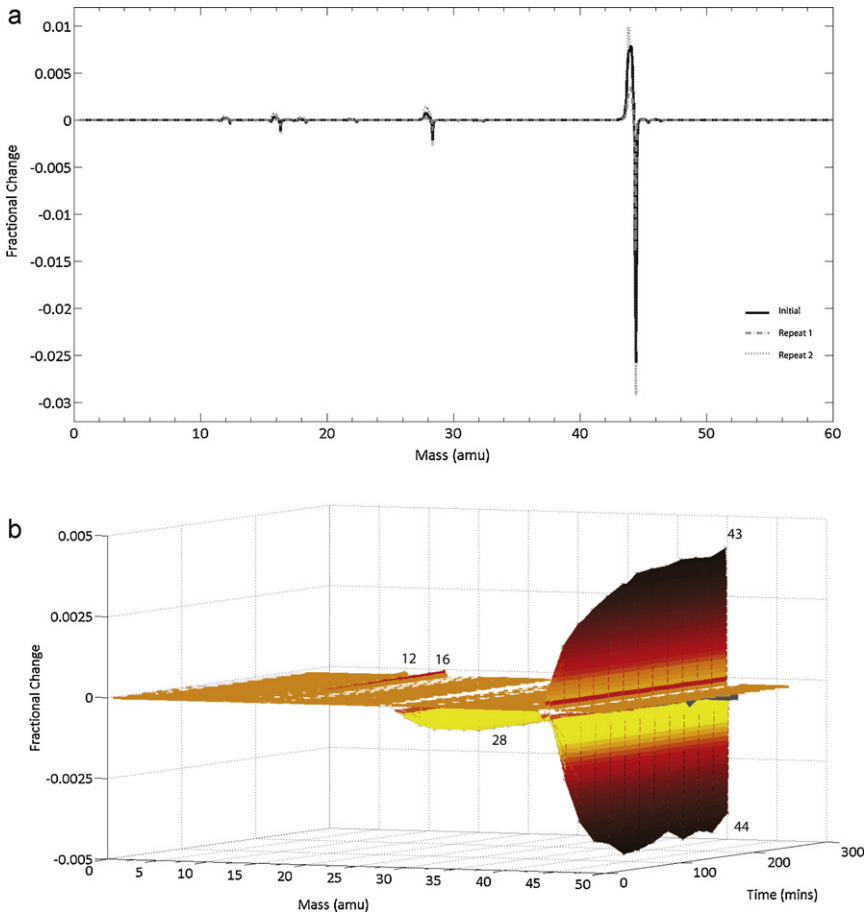

Fig. 6. The influence of water on the reaction. The change in the composition shows a similar change to that seen within the reaction that is unwashed.

4.2. Discussion of the effects of the stabilisation of the surface

TiO_2 in its anatase form has a tetragonal, ditetragonal dipyramidal, mineral structure. This results, on the surface, in the formation of both five (5f) and six fold co-ordinated (6f) Ti atoms and two (2f) and three fold co-ordinated (3f) oxygen atoms. This leads to a saw tooth surface consisting of acidic basic pair of unsaturated Ti_4^+ 5f linked by O_2^- 2f bridging pairs interspersed with fully saturated Ti 6f and O 3f pairs [16–18]. Using Paulings second rule, the valency of an ion is equal to the sum of the electrostatic bond strength of the adjacent ions surrounding it [19]. It is possible to consider the two different types of oxygen atom, and the corresponding relative

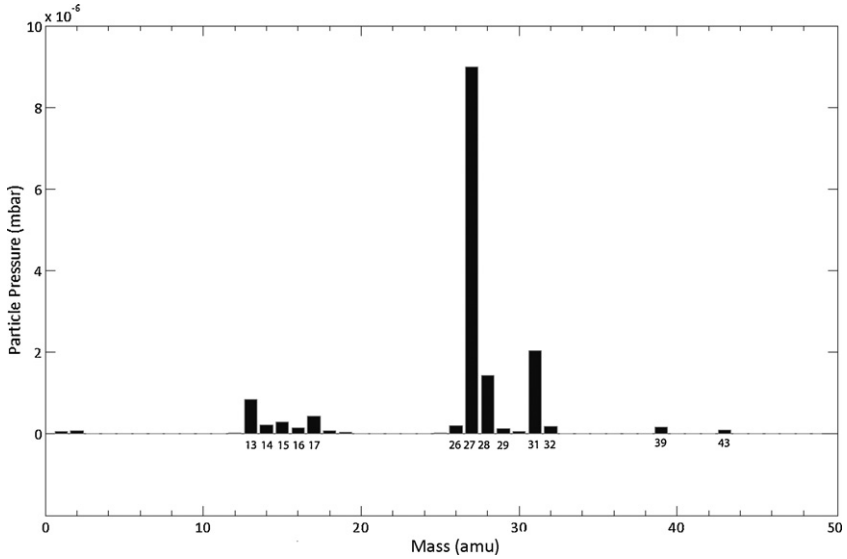

Fig. 7. Showing the composition of the main formed product. Major electron impact (EI) ionization splitting peaks are ascribed to C_2H_3 (27), CO (28), CH_3O (31) and $C_2H_3O^-$ (43).

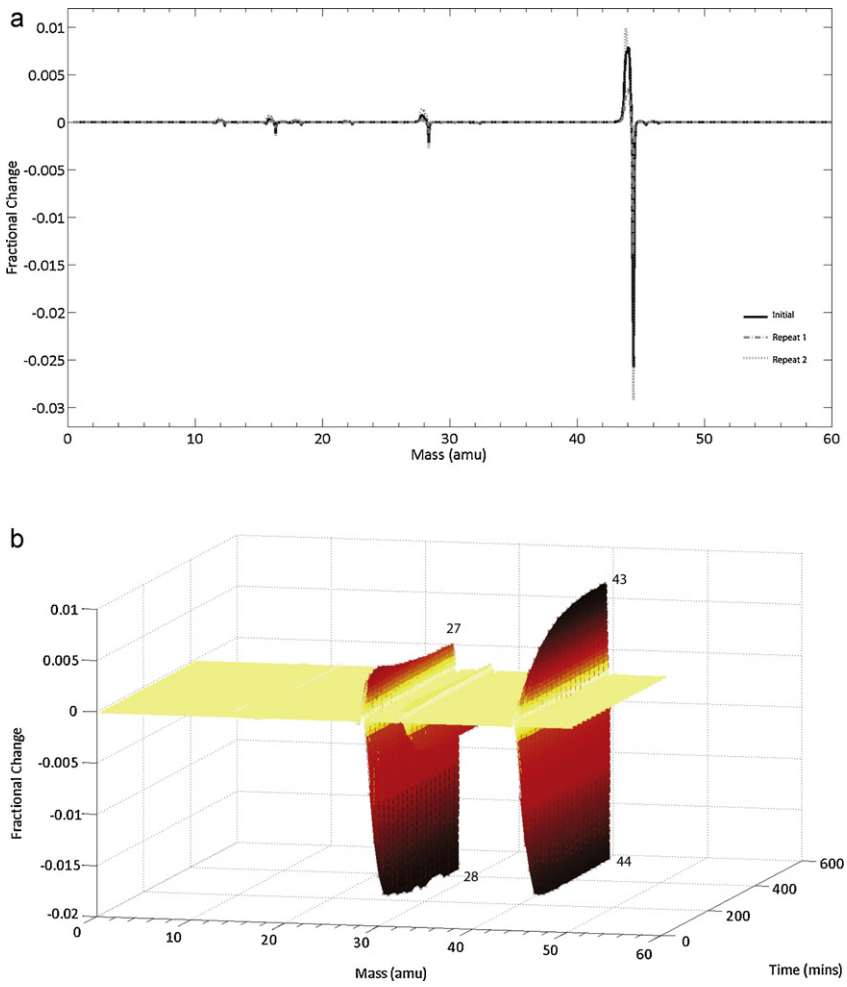

Fig. 8. The influence of soft X-rays on the reaction.

bond strength each draws as an approximation for the reactivity of the surface. This can be also be used to compare relative changes and proton affinity of surface oxygen. Considering a fully saturated Ti 6f and O 3f pair, Ti is donating a +4 charge over 6 O atoms, i.e. each a +2/3 charge. The O 3f gains three times this charge so thus is has a +2 electrostatic charge and so is neutral. Considering an unsaturated Ti 5f, O 2f pair then the Ti is donating a +4 charge over 5 O atoms i.e. each +4/5 charge. This results in the O atom carrying a relative −2/5 charge deficiency, when relaxed. As is well documented [12] the surface of the TiO_2 molecule will interact with UV light to produce an electron hole in the valance band. This electron hole can interact with the adsorbed molecules, changing the charge surface to an effective +3/5. Compounds with high electron density, including those such as $C_2H_3O^-$, will interact with this electron hole and stabilise the structure. The negative charge carried by the molecule can stabilise the excess hole, and in turn this can stabilise

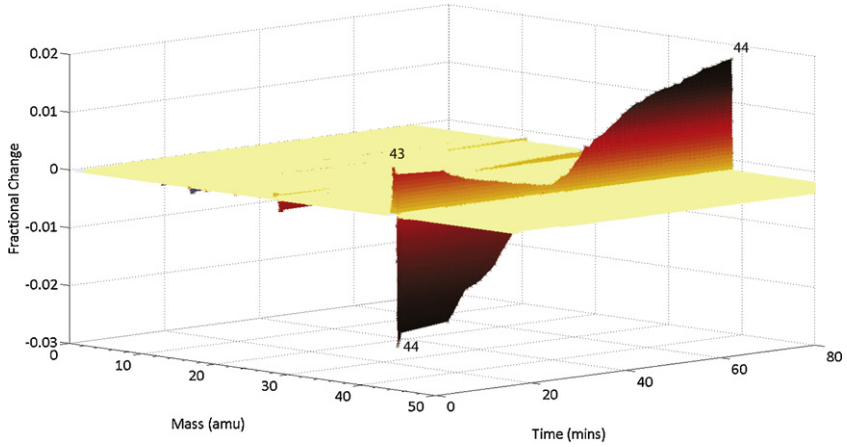

Fig. 9. Showing the changes in gas composition over time without illumination, a near complete reversion is seen after 100 min, although a small proportion of stable intermediates remain

the heavily strained bond. When the illumination of the surface is ceased the electron holes will no longer form. This will lead to the carbonyl compounds interacting with the hole, being desorbed and broken down (Fig. 9).

4.3. Reaction mechanics

The major increase detected in the gas phase in each experiment was ascribed to the formation of $C_2H_3O^-$, ethenolate (mass 43). The other species generated during the experiment (CO, CH_4, C) were considered to represent more stable (i.e. non free radical) bi-products of the photocatalytic reduction, illustrated by their persistence after the cessation of illumination. From this a possible reaction mechanism is described in the following series of reactions:

$$TiO_2 \xrightarrow{h\nu} h^+_{vb} + e^-_{cb} \quad (2a)$$

$$h^+_{vb} + H_2O \longrightarrow {}^\bullet OH + H^+ \quad (2b)$$

$$e^-_{cb} + H^+ \longrightarrow {}^\bullet H \quad (2c)$$

$$CO_2 + e^-_{cb} \longrightarrow {}^\bullet CO_2^- \quad (2d)$$

$${}^\bullet CO_2^- + {}^\bullet H \longrightarrow C + OH^- \quad (2e)$$

$$CO + e^-_{cb} \longrightarrow {}^\bullet CO^- \quad (2f)$$

$${}^\bullet CO^- + {}^\bullet H \longrightarrow C + OH^- \quad (2g)$$

$$OH^- + h^+_{vb} \longrightarrow {}^\bullet OH \quad (2h)$$

$${}^\bullet OH + h^+_{vb} \longrightarrow H^+ + \frac{1}{2}O_2 \quad (2i)$$

$${}^\bullet OH + {}^\bullet H \longrightarrow H_2O \quad (2j)$$

$${}^\bullet C + {}^\bullet H \longrightarrow {}^\bullet CH \quad (2k)$$

$${}^\bullet CH + {}^\bullet H \longrightarrow CH_2 \quad (2l)$$

$$CH_2 + {}^\bullet H \longrightarrow {}^\bullet CH_3 \quad (2m)$$

$${}^\bullet CH_3 + {}^\bullet CO^- \longrightarrow C_2H_3O^- \quad (2n)$$

The mechanisms have been proposed previously [4,14,20,21] with the reactive sequence considered to produce methane (CH_4) and hydrogen (H_2) as major products.

In the mechanism presented by Eqs. (2a)–(2n), the TiO_2 absorbs a photon of light ($h\nu$) generating an electron in the conductive band and a corresponding hole in the valence band on the surface (2a). The hole will interact with the H_2O that is adsorbed to the surface, generating the highly reactive •OH radical (2b). The corresponding H^+ ion will interact with the free electron to produce a •H radical (2c). Furthermore CO_2 will interact with the free electrons to produce ${}^\bullet CO_2^-$ radicals (2d). It is then possible for this to combine with a •H radical, with the formation of the stable intermediate CO, corresponding to the increase in mass 28 that is observed. The CO can then go on to interact with a further free electron to produce a ${}^\bullet CO^-$ radical (2f), which in turn can interact with a •H radical to give stable C (2g) shown to build up and poison the catalysis surface over time. It is possible for the generated OH^- to either directly combine with H^+ or with and electron hole and a •H (h,i) to reproduce H_2O. The C can be built up by the addition of •H radicals to the ${}^\bullet CH_3$ radical (2k–m). To form the $C_2H_3O^-$ the ${}^\bullet CH_3$ radical interacts with the ${}^\bullet CO^-$ form (2f) to produce the end product (2n). The excess ${}^\bullet OH^-$ ions generated in (2e,g) can be converted back to •H radicals by (2h,i,c). The overall reaction equates to:

$$2CO_2 + \frac{3}{2}H_2O \xrightarrow{9h^+_{vb}+10e^-_{cb}} C_2H_3O^- + \frac{9}{2}O_2 \quad (3a)$$

There is a partial pressure increase of 2 molecules associated with the above reaction (3a), and there is no associated loss of water out of the gas phase. However, there is an increase in the amount of O in the system and significant raise in CO and C in the reaction path way. The overall reactions for these are summarised by Eqs. (4a) and (4b).

$$CO_2 \xrightarrow{2h^+_{vb}+2e^-_{cb}} CO + \frac{1}{2}O_2 \quad (4a)$$

$$CO_2 \xrightarrow{4h^+_{vb}+4e^-_{cb}} C + O_2 \quad (4b)$$

These also produce more O_2 which offsets partial pressure drops related to other reactions and maintains overall system pressure. From the data it can be determined that 11 times as much $C_2H_3O^-$ is produced as CO and C combined. This is equivalent, in terms of pressure, as these reactions generate excess pressure and the products are likely to fill the adsorption sites of the H_2O. The equilibrium gas composition achieved in the system after 250 min of illumination is considered to represent a balance between production of new $C_2H_3O^-$ on the titania surface and spontaneous decomposition of the gaseous $C_2H_3O^-$. The H_2O for the reaction is likely to come off the adsorbed surface as opposed to the gas phase. It is likely that these sites are then left either vacant or adsorbed with the formed product, O_2. Thus the overall increase in O_2 is less than is normally observed as most is likely to be adsorbed to the surface.

4.4. X-ray

It has been well documented that with UV illumination TiO_2 can be excited to act photocatalytically, with the band gap of a material determining the minimum energy required to promote an electron to the conduction band [12]. The current work provides a clear demonstration that photocatalytic behaviour in TiO_2 may also be induced using soft X-ray irradiation. It is considered that when irradiated with a higher energy photon the TiO_2 electrons are promoted to a higher energy level. These are available in the same manner for interactions with adsorbed molecules. Results show only a minor difference in formation products, with more $C_2H_3O^-$ formed by X-ray exposure, as (presumably) shadowing effects are eliminated. It is also postulated this may be due to the influence of higher energy electrons being able to facilitate alternative reaction pathways. Greater rates of catalysis poisoning are also observed on the titania surface with X-ray illumination. The exact mechanism for X-ray activation is beyond the scope of this paper and will be a focus of further research.

5. Conclusions

The present study has tested the capability of nano-TiO_2 coated surfaces for the reduction of CO_2 in the gas phase. The results clearly indicate that it is possible to reduce CO_2 on TiO_2 with a relatively short time to achieve an equilibrium state. Further work would be required in three main areas in order to use TiO_2 as a material for CO_2 sequestration. Firstly, the catalyst would require band gap modification in order to be active under visible light and therefore able to be formed into a passive system. Secondly, the reaction product would have to be modified in order to form a stable product that could be removed and processed further. Finally, a method to overcome catalysis poisoning would have to be developed.

From this study the following key conclusions have been drawn:

- Under continuous UV illumination within a closed system and in the presence of H_2O, TiO_2 surfaces are observed to transform CO_2 through photocatalytic reduction forming $C_2H_3O^-$ as a major product. The amount of product produced is increased 2-fold by adopting a mixed phase system.

- The product is observed to be surface stabilised, reverting predominantly and gradually to CO_2 achieving complete decomposition within 100 min of ceasing illumination.
- Irradiation with soft X-rays was also found to activate TiO_2 and reduce CO_2 on the surfaces in a similar manner to that seen for UV illumination. This has significant implications for other studies beyond the scope of this work.

Acknowledgements

We would like to thank Mr John Nicholson, for his excellent technical assistance in this project, and to Prof. Geoffrey Allen for his guidance and support.

References

[1] D.S. Solomon, Z. Qin, M. Manning, M.M. Chen, K. Averyt, M. Tignor, H. Miller (Eds.), Contribution of Working Group I to the Fourth Assessment Report of the Intergovernmental Panel on Climate Change, 2007, Cambridge University Press, Cambridge, United Kingdom, 2007.
[2] M. Parry, O. Canziani, J. Palutikof, P. van der Linden, C. Hanson (Eds.), Contribution of Working Group II to the Fourth Assessment Report of the Intergovernmental Panel on Climate Change, 2007, Cambridge University Press, Cambridge, United Kingdom, 2007.
[3] C. Hepburn, N. Stern, A new global deal on climate change, Oxford Review of Economic Policy 24 (2008) 259–279.
[4] M. Anpo, H. Yamashita, Y. Ichihashi, S. Ehara, Photocatalytic reduction of CO_2 with H_2O on various titanium oxide catalysts, Journal of Electroanalytical Chemistry 396 (1995) 21–26.
[5] T. Mizuno, K. Adachi, K. Ohta, A. Saji, Effect of CO_2 pressure on photocatalytic reduction of CO_2 using TiO_2 in aqueous solutions, Journal of Photochemistry and Photobiology A: Chemistry 98 (1996) 87–90.
[6] S. Kaneco, H. Kurimoto, K. Ohta, T. Mizuno, A. Saji, Photocatalytic reduction of CO_2 using TiO_2 powders in liquid CO_2 medium, Journal of Photochemistry and Photobiology A: Chemistry 109 (1997) 59–63.
[7] M. Anpo, H. Yamashita, K. Ikeue, Y. Fujii, Y. Ichihashi, S.G. Zhang, D.R. Park, S. Ehara, S.-E. Park, J.-S. Chang, J. Whan Yoo, M.A.K.I.S.Y.T. Inui, T. Yamaguchi, Photocatalytic Reduction of CO_2 with H_2O on Titanium Oxides Anchored within Zeolites, Studies in Surface Science and Catalysis, vol. 114, Elsevier, pp. 177–182.
[8] S. Kaneco, Y. Shimizu, K. Ohta, T. Mizuno, Photocatalytic reduction of high pressure carbon dioxide using TiO_2 powders with a positive hole scavenger, Journal of Photochemistry and Photobiology A: Chemistry 115 (1998) 223–226.
[9] K.R. Szulczyk, B.A. McCarl, G. Cornforth, Market penetration of ethanol, Renewable and Sustainable Energy Reviews 14 (2010) 394–403.
[10] A. Dagoumas, G. Papagiannis, P. Dokopoulos, An economic assessment of the Kyoto protocol application, Energy Policy 34 (2006) 26–39.
[11] S. Barrett, Political economy of the Kyoto protocol, Oxford Review of Economic Policy 14 (1998) 20–39.
[12] O. Carp, C.L. Huisman, A. Reller, Photoinduced reactivity of titanium dioxide, Progress in Solid State Chemistry 32 (2004) 33–177.
[13] J.A. Herrera Melián, J.M. Doña Rodríguez, A. Viera Suárez, E. Tello Rendón, C. Valdés do Campo, J. Arana, J. Pérez Peña, The photocatalytic disinfection of urban waste waters, Chemosphere 41 (2000) 323–327.
[14] G.R. Dey, Chemical reduction of CO_2 to different products during photo catalytic reaction on TiO_2 under diverse conditions: an overview, Journal of Natural Gas Chemistry 16 (2007) 217–226.
[15] P.S. Marcos, J. Marto, T. Trindade, J. Labrincha, Screen-printing of TiO_2 photocatalytic layers on glazed ceramic tiles, Journal of Photochemistry and Photobiology A: Chemistry 197 (2008) 125–131.
[16] A. Selloni, A. Vittadini, M. Grätzel, The adsorption of small molecules on the TiO_2 anatase (1 0 1) surface by first-principles molecular dynamics, Surface Science 402–404 (1998) 219–222.
[17] T. Homann, T. Bredow, K. Jug, Adsorption of small molecules on the anatase (1 0 0) surface, Surface Science 555 (2004) 135–144.
[18] J. Scaranto, S. Giorgianni, Adsorption of difluoromethane on titanium dioxide: investigation of the FTIR spectra and quantum-mechanical studies of the adsorbate-substrate structures, Spectrochimica Acta Part A: Molecular and Biomolecular Spectroscopy 74 (2009) 1072–1076.
[19] K. Tkacz-Smiech, A. Kolezynski, W.S. Ptak, Pauling's electrostatic rule for partially covalent/partially ionic crystals, Journal of Physics and Chemistry of Solids 61 (2000) 1847–1853.
[20] S.S. Tan, L. Zou, E. Hu, Photocatalytic reduction of carbon dioxide into gaseous hydrocarbon using TiO_2 pellets, Catalysis Today 115 (2006) 269–273.
[21] K. Kocí, L. Obalová, L. Matejová, D. Plachá, Z. Lacný, J. Jirkovský, O. Solcová, Effect of TiO_2 particle size on the photocatalytic reduction of CO_2, Applied Catalysis B: Environmental 89 (2009) 494–502.